A multiple-frequency method for potentially improving the accuracy and precision of *in situ* target strength measurements

David A. Demer
Southwest Fisheries Science Center, P.O. Box 271, La Jolla, California 92038

Michael A. Soule
Sea Fisheries Research Institute, Private Bag X2, 8012 Rogge Bay, Cape Town, South Africa

Roger P. Hewitt
Southwest Fisheries Science Center, P.O. Box 271, La Jolla, California 92038

(Received 11 May 1998; revised 13 November 1998; accepted 4 January 1999)

The effectiveness of a split-beam echosounder system to reject echoes from unresolvable scatterers, thereby improving the measurements of *in situ* target strengths (TS) of individuals, is dramatically enhanced by combining synchronized signals from two or more adjacent split-beam transducers of different frequencies. The accuracy and precision of the method was determined through simulations and controlled test tank experiments using multiple standard spheres and 38- and 120-kHz split-beam echosounders. By utilizing the angular positional information from one of the split-beam transducers, additional corresponding TS measurements were shown to be obtainable from a juxtaposed single-beam transducer. Both methods were utilized to extract *in situ* TS measurements of Antarctic scatterers simultaneously at 38, 120, and 200 kHz. The ultimate efficiency of the multiple-frequency method is shown to be limited by phase measurement precision, which in turn is limited by the scattering complexity of targets, the signal-to-noise ratio, and the receiver bandwidth. Imprecise phase measurements also result in significant beam-compensation uncertainty in split-beam measurements. Differences in multi-frequency TS measurements provided information about the identity of constituents in a mixed species assemblage. The taxa delineation method has potential, but is limited by compounding measurement uncertainties at the individual frequencies and sparse spectral sampling.
[S0001-4966(99)01204-7]

PACS numbers: 43.60.Qv, 43.30.Vh, 43.30.Xm [JCB]

INTRODUCTION

A distribution of backscattering cross-sectional areas of individual scatterers ($P\{\sigma_{bs}\}$) is a critical factor in the estimation of animal density (numbers/km^2) from an acoustical survey (Bodholt, 1990; Hewitt and Demer, 1993). Measurements of σ_{bs} (m^2/animal), frequently expressed as target strength [$TS = 10\log(\sigma_{bs})$], can be made either in their natural state and environment (*in situ*) or through controlled experimentation (Ehrenberg, 1989). However, the TS of fish and zooplankton are highly dependent upon the variation of sound scattering with animal size, shape, orientation, and acoustic impedance (Chu *et al.*, 1992; Stanton *et al.*, 1994; Demer and Martin, 1995). Thus, the applicability of TS measurements made on constrained, sedated, or dead animals may be suspect. On the other hand, efforts to make direct *in situ* TS measurements have been hindered by equipment and physical limitations (Ehrenberg, 1979; Foote, 1991). This study aims to improve the methods for measuring TS *in situ*, concurrent with echo-integration surveys, by requiring simultaneously detected echoes to pass multiple-target rejection algorithms at two or more frequencies. Additionally, the simultaneous measurements of TS at multiple frequencies are used to empirically characterize the frequency-dependent scattering or ''acoustic signatures'' of some species. In some cases, the latter may permit acoustical identification of taxa and the apportionment of total echo energy to different species.

The echosounder used in this study is the three-frequency Simrad EK500 (Bodholt *et al.*, 1988). A series of simulations (Sec. I) and test tank experiments (Sec. II) were conducted to (1) characterize the precision of TS measurements made with the EK500 at 38 and 120 kHz; (2) evaluate the adequacy of the EK500 single-frequency algorithm for rejecting multiple targets in some situations; and (3) demonstrate that the individual scatterers are more accurately delineated by matching the outputs of the EK500 algorithm at two or more frequencies. Field experiments (Sec. III) were then conducted to demonstrate the efficacy of the new method for accurately and simultaneously measuring *in situ* TS measurements of individual scatterers at three frequencies (38, 120, and 200 kHz). With adjacently mounted transducers, the target-position information from the split-beam systems was used to derive beam-compensated TS values from the 200-kHz single-beam system (Demer, 1994). Finally, differences in the simultaneous TS measurements were used to relate the acoustic measurements to the species composition of net samples.

In the following paragraphs, several terms or concepts (animal density, split-beam measurements, noise effects, single target detections, and taxa delineation) are described as they pertain to fisheries acoustics theory and instrumentation.

A. Animal density estimation

In acoustical surveys of aquatic organisms, the areal density of scatterer type ''x'' (ρ_x) can be estimated from the integrated volume backscattering strength (S_{A_x}), or the total backscattering cross-sectional area per unit of sea-surface area (m^2/km^2) from type-x animals, divided by the frequency-weighted backscattering cross-sectional area from an individual type-x animal ($P\{\sigma_{\mathrm{bs}_x}\}\cdot\sigma_{\mathrm{bs}_x}$). In practice, a discrete sum form of the probability density function (PDF) is used:

$$\rho_x = S_{A_x} \Big/ \sum_{i_x=1}^{n_2} f_{x_i}\sigma_{\mathrm{bs}_{x_i}}, \tag{1}$$

where f_{x_i} is the relative frequency of type-x animals with $\sigma_{\mathrm{bs}_{x_i}}$, such that $\Sigma_{i_x=1}^{n_x} f_{x_i}=1$, where i_x refers to the ith class of σ_{bs_x} and n_x is the number of σ_{bs}-classes of type-x animals.

B. Split-beam measurements

During the survey, *in situ* TS measurements of individual scatterers are possible using a split-beam echosounder to locate echoes in three-dimensional space and a method for excluding unresolvable targets. A sound pulse is transmitted simultaneously from four quadrants of a split-beam transducer and received by each quadrant individually. The electrical phase between the signals received from two halves of the transducer (ϕ_e) is related to the angle between the beam-axis and the target (θ):

$$\phi_e = kd_{\mathrm{eff}}\sin\theta, \tag{2}$$

where k is the acoustic wave number and d_{eff} is the effective separation between two transducer halves (a function of element shading). In the alongship plane, $\theta=\alpha$ and $d_{\mathrm{eff}}=d_\alpha$ and in the athwartship plane, $\theta=\beta$ and $d_{\mathrm{eff}}=d_\beta$. The angular resolution of the system (ζ) is determined by differentiating ϕ_e with respect to θ:

$$\zeta = \frac{\Delta\phi_e}{kd_{\mathrm{eff}}\cos\theta}, \tag{3}$$

and evaluating with the phase resolution of the echosounder (in the case of the EK500, $\Delta\phi_e=180$ electrical degrees per 64 phase steps), a small angle approximation ($\cos\theta\cong 1$), and the transducer angle sensitivity ($\Lambda=kd_{\mathrm{eff}}$):

$$\zeta \cong \left(2.8125\left(\frac{\text{electrical degree}}{\text{phase step}}\right)\right) \Big/ \left(\Lambda\left(\frac{\text{electrical degree}}{\text{spatial degree}}\right)\right). \tag{4}$$

The radial range to the target ($r=ct_{2\text{-way}}/2$) is estimated from the sound speed (c) and half of the two-way propagation delay ($t_{2\text{-way}}$). Uncertainty in the determination of $t_{2\text{-way}}$ is affected by the echo pulse rise time and a small delay in the receiving electronics (MacLennan, 1987). Therefore, $t_{2\text{-way}}$ is most accurately estimated by subtracting the system-dependent receiver delay (t_{del}) from the propagation delay (t_h) measured between the start of the transmit pulse and the point on the leading edge of the echo at which the amplitude has risen to half the peak value (MacLennan and Simmonds, 1992; Fernandes and Simmonds, 1996).

Thus, the split-beam system allows an individual animal to be located in three-dimensional space (α, β, and r), provided that it is separated from other scatterers by a radial distance greater than the range resolution or half the product of c and the pulse duration (τ) (MacLennan and Simmonds, 1992). Of course, the echo amplitude must also exceed the detection threshold. In this case, the backscattering cross-sectional area of an individual scatterer can be estimated from the ratio of the received power (p_r) to the transmit power (p_t), with compensations for spherical spreading, absorption, system gain, and the transducer beam pattern (Kerr, 1988; Simrad, 1996):

$$\sigma_{\mathrm{bs}} = \frac{p_r 16\pi^2 r^4 10^{2\gamma r}}{p_t g_0^2 r_0^2 \lambda^2}\cdot b(\alpha,\beta)^2, \tag{5}$$

where γ is the absorption coefficient (dB/m), g_0 is the system gain on the beam axis, r_0 is the reference distance (1 m), and $b(\alpha,\beta)$ is the one-way beam pattern compensation evaluated in the direction of the target [$b(\alpha,\beta)\geqslant 0$]. In logarithmic form,

$$\begin{aligned}\mathrm{TS} = {} & P_r + 20\log(4\pi) + 40\log(r) + 2\gamma r - P_t - 2G_0 \\ & - 20\log(\lambda) + 2B(\alpha,\beta),\end{aligned} \tag{6}$$

where the decibel forms of p_t, p_r, g_0, and $b(\alpha,\beta)$ are P_t, P_r, G_0, and $B(\alpha,\beta)$, respectively (dB *re*: 1 W). The first seven terms of (6) are collectively termed the uncompensated target strength (TS_U):

$$\mathrm{TS} = \mathrm{TS}_U + 2B(\alpha,\beta). \tag{7}$$

Knowing the off-axis angles and the shape of the beam, compensation can be applied to normalize all TS measurements to the calibrated beam axis.

C. Noise effects

As with all acoustical measurements, background noise (e.g., thermal, wind, bubble, engine, tank boundary reverberation, etc.) can affect both the accuracy and precision of the phase measurements and thus the estimates of off-axis angles. The total sound pressure (p) is the sum of the complex signal (p_s) and the complex noise (p_n), with time-varying amplitudes [$P_s(t)$ and $P_n(t)$, respectively]:

$$p_s = P_s(t)e^{j\omega t} = P_s(t)(\cos(2\pi ft) + j\sin(2\pi ft)), \tag{8}$$

$$p_n = P_n(t)e^{j\omega t} = P_n(t)(\cos(2\pi ft) + j\sin(2\pi ft)), \tag{9}$$

$$\begin{aligned} p &= (P_s(t) + P_n(t))e^{j\omega t} \\ &= (P_s(t) + P_n(t))(\cos(2\pi ft) + j\sin(2\pi ft)).\end{aligned} \tag{10}$$

The phase estimate from the qth quadrant ($\hat{\phi}_{e_q}$) is determined by the arctangent of the imaginary part of the total received pressure divided by the real part (Senturia and Wedlock, 1975). Assuming the signal has zero phase (arbitrary reference) and a constant amplitude which is much greater than the noise level [$P_s \gg P_n(t)$], a small angle approximation can be employed [$\tan^{-1}(\phi_{e_q})\cong\phi_{e_q}$], and the phase estimate can be approximated by

TABLE I. Minimum SNR (dB) to estimate off-axis angles ($\hat{\theta}=\alpha$ or β) which are precise (95% confidence interval) to within one to five quantization steps ($\Delta\phi_e$). The requisite SNR decreases as the number of phase samples (Z) in the average phase difference estimate ($\overline{\Delta\hat{\phi}}$) increases. The basic sampling rates of the EK500 are 7.5, 25, and 37.5 kHz at 38, 120, and 200 kHz, respectively. Therefore, for pulse durations of 1.0 ms at 38 kHz and 0.3 ms at 120 kHz, approximately seven samples are averaged and a SNR of 24 dB is required for maximum precision in the phase measurements.

Minimum signal-to-noise ratio (dB)				SNR for phase estimate ($\Delta\hat{\phi}_e$)	SNR for average estimated phase ($\overline{\Delta\hat{\phi}_e}$)								
Phase (θ)				Samples in average (Z)									
Radians ($s\Delta\phi_e$)	Degrees (ES3812)	Degrees (ES120-7)	Steps (s)	1	2	3	4	5	6	7	8	9	10
0.049	0.23	0.13	1	32	29	27	26	25	24	24	23	23	22
0.098	0.45	0.27	2	26	23	21	20	19	18	18	17	17	16
0.147	0.68	0.40	3	23	20	18	17	16	15	14	14	13	13
0.196	0.90	0.54	4	20	17	15	14	13	12	12	11	11	10
0.245	1.13	0.67	5	18	15	13	12	11	10	10	9	9	8

$$\hat{\phi}_{e_q} \cong \frac{P_n(t)\sin(2\pi ft)}{P_s\cos(2\pi ft)}. \tag{11}$$

Assuming the noise is Gaussian with root mean square (rms) intensity σ_n^2 (Greenlaw and Johnson, 1983), and recalling that $\mathrm{var}[Cx]=C^2\,\mathrm{var}[x]$, the variance of the phase estimate is

$$\mathrm{var}[\hat{\phi}_{e_q}]=\mathrm{var}\left[\frac{P_n\sim N(\overline{x},\sigma_n^2)}{P_s}\right]=\frac{1}{P_s^2}\mathrm{var}[P_n(t)]=\frac{\sigma_n^2}{P_s^2}, \tag{12}$$

and the signal-to-noise power ratio (snr) is

$$\mathrm{snr}=\frac{P_s^2}{2\sigma_n^2}. \tag{13}$$

The variance of the single-channel phase estimate is determined by solving (13) for σ_n, substituting into (12):

$$\mathrm{var}[\hat{\phi}_{e_q}]=\frac{1}{2\ \mathrm{snr}}. \tag{14}$$

To measure phase in the EK500, the four receiver channels are amplitude limited to allow comparison of the delay between zero crossings for phase determination. The measured delays are interpreted in firmware as phase differences between half-beams. Depending upon the clock-rate and the algorithm, more than one estimate of single-channel phase may be averaged for each estimate of the phase difference between half-beams. Moreover, relative phases may be more precisely determined by cross correlation (Medwin and Clay, 1998). Conservatively, however, assume that each phase-difference estimate ($\Delta\hat{\phi}_e$) is determined from two unaveraged estimates of single-channel phase ($\hat{\phi}_{e_1}-\hat{\phi}_{e_2}$); therefore, $\mathrm{var}(\Delta\hat{\phi}_e)=2\,\mathrm{var}(\hat{\phi}_{e_q})$. The actual phase estimates are averages of Z independent phase difference estimates made within the -6-dB points of the echo envelope ($\overline{\Delta\hat{\phi}_e}=(\Sigma_Z(\Delta\hat{\phi}_e)_Z)/Z$) and $\mathrm{var}[\overline{\Delta\hat{\phi}_e}]=\mathrm{var}[\Delta\hat{\phi}_e]/Z=(2/Z)\cdot\mathrm{var}[\hat{\phi}_{e_q}]$ (Rice, 1988). Thus, for maximum precision of the mean phase difference between half-beams, the phase quantization of the echosounder ($\Delta\phi_e=0.0491$ radians/phase step) must be greater than $2\cdot sd[\hat{\phi}_{e_q}]$ (95% confidence interval):

$$\mathrm{SNR}>10\log\left(\frac{4}{Z(s\Delta\phi_e)^2}\right), \tag{15}$$

where $\mathrm{SNR}=10\log(\mathrm{snr})$ in decibels (dB) and s is the integer number of phase steps. For maximum precision, s is 1. If reduced precision is acceptable, (15) can be evaluated with increased numbers of phase steps (Table I).

D. Single-target detection

In order to reject returns from unresolvable targets, a multi-tiered algorithm can be employed (Bodholt, 1991; Bodholt and Solli, 1992). As implemented in the EK500 Echosounder (Simrad, 1996), filters are imposed on the minimum TS, the minimum and maximum duration of the echo envelope (echo width at -6-dB points normalized by τ), maximum $B(\alpha,\beta)$, and the maximum sample-to-sample deviation of the phase measurements (Table II). The constraint on the minimum normalized echo length is intended to reject noise and destructively interfering echoes from multiple targets with different bearings but similar ranges. The maximum normalized echo length criteria is intended to eliminate overlapping echoes from multiple targets at similar bearings, but different yet unresolvable ranges. The maximum gain compensation is intended to reduce biases due to thresholding of smaller targets at the beam periphery (reduced sensitivity), and a decrease in the accuracy of the estimated beam compensation function $[\hat{B}(\alpha,\beta)]$ at large off-axis angles. The maximum phase deviation is employed to reject incoherent echoes from unresolvable target multiples. In the EK500 firmware versions 5.0 and later, an improved phase deviation classifier (P_{dev}) is employed which is simply the standard deviation of the phase samples within the echo length (Soule *et al.*, 1997).

Unfortunately, the multiple-target rejection algorithm is sometimes imperfect at high scatterer densities (Hewitt and Demer, 1991). This is especially true when constructive-interference results from multiple scatterers residing in the

TABLE II. Multiple-target rejection criteria used in both the tank and field experiments. Unresolvable targets are filtered, to some extent, by imposing (1) a minimum target strength (Min. TS); (2) minimum and maximum duration of the echo envelope, normalized by the pulse duration (τ); (3) maximum one-way beam compensation (Max. B); and (4) a maximum sample-to-sample deviation of the phase measurements (P_{dev}).

Minimum target strength (TS)	-90 dB
Minimum echo length	0.8τ (s)
Maximum echo length	1.5τ (s)
Maximum beam compensation [$B(\alpha,\beta)$]	4 dB[a]
Maximum phase deviation (P_{dev})	4 steps[a]

[a]Not applicable for single-beam system.

same resolution volume (Soule *et al.*, 1995, 1996); their simulations and tank measurements showed that overlapping echoes from targets separated by half-multiples of a wavelength were preferentially accepted. However, because the interference is dependent upon the relationships between acoustic wavelength ($\lambda = c/f$) and scatterer spacing, the effects vary with frequency (Foote, 1996). In other words, for the range separation between two targets (Δr) to be equal to an integer multiple of $\lambda/2$ at two different discrete frequencies simultaneously, one wavelength (λ_1) must be M/N times the other wavelength (λ_2), where M and N are both integers. This occurs very infrequently. For example, at the precise EK500 frequencies of 37.879 and 119.048 kHz, a sound speed (c) of 1500 m/s, pulse lengths of 1.0 ms, and transducer beamwidths of 7.0°, this exact situation does not occur within the resolution volume, bounded by the pulse width and the transducer -3-dB points, to a maximum range of 250 m. Compromising this ideal situation are the finite bandwidths of the pulsed transmissions ($\cong 1$ kHz) which may still allow interference to occur when target spacing is slightly more or less than a half-wavelength of the center frequency. Nevertheless, it follows that the accuracy and precision of *in situ* TS measurements can likely be improved by requiring simultaneously detected echoes to pass multiple target rejection algorithms at two or more frequencies.

E. Taxa delineation

In addition to reducing measurement uncertainty, simultaneous measurements of *in situ* TS at more than one frequency may provide enough information to identify scatterers. Holliday (1977) showed that biophysical information could be extracted from multi-frequency acoustic backscatter. Greenlaw (1979) then proposed, and Madureira *et al.* (1993) and Brierly *et al.* (submitted) demonstrated, that differences in volume backscattering strength measured at multiple frequencies could be used to classify scatterer sizes. Greenlaw's method was also adapted to multi-frequency *in situ* TS measurements, and coupled with distributions of theoretical expectations (e.g., $P\{\sigma_{120} - \sigma_{38\text{ kHz}}\}$), to estimate taxa of individual scatterers (Demer, 1994).

I. SIMULATIONS

The potential utility of the multiple-frequency method for rejecting echoes from multiple unresolvable targets was first tested with a simulation similar to that conducted in Soule *et al.* (1996). Two unresolvable targets were randomly and independently positioned within a three-dimensional pulse resolution volume (at 120 kHz), and assigned a point-location in a spherical coordinate system ($10.0 \leqslant r \leqslant 10.75$ m; 0 degrees$\leqslant$polar angle$\leqslant$3 degrees; and 0 degrees$\leqslant$azimuth angle $\leqslant$360 degrees). Transmitted pulses were simulated at both 38 and 120 kHz by multiplying a Gaussian envelope and a continuous sine wave at each frequency. The band-limited pulses had amplitudes of unity and were approximately 1.0 ms between -6-dB points. The complex echo waveforms were computed as received by each quadrant of collocated 38 and 120 kHz split-beam transducers. The transmission losses were neglected and the sampling rates were chosen to be equivalent to the EK500 (7.5 and 25 kHz, respectively). Both transducers were modeled as point-receivers with ideal beams. Ignoring shading, quadrant separations of 138.5 and 55 mm resulted in angle sensitivities of 21.9 and 23.8 at 38 and 120 kHz, respectively.

At each frequency, the reflected pressure waves received at each of the four transducer elements ($q = 1$, 2, 3, or 4) from each of the two randomly located targets ($l = 0$, 1, or 2) is given by Soule *et al.* (1996):

$$p_{q1}(t) = \sigma_{\text{bs}_1}^{1/2} \cdot e^{(-[t-((r_{q1}+r_1)/c)]^2/2T_p^2)} \cdot e^{j(\omega t-(r_{q1}+r_1)k)}, \qquad (16)$$

where σ_{bs_1} is the backscattering cross-sectional area of the lth target, r_{q1} is the range from element q to target 1, r_1 is the range from the origin to target l, $c = 1500$ m/s, j is the imaginary number ($\sqrt{-1}$), T_p is the pulse width parameter (0.4 ms) used to set the duration of the Gaussian envelope, k is the wave number ($2\pi c/f$), and the radian frequency ($\omega = 2\pi f$) is assumed to be a constant for narrow bandwidth operation. Individual backscattering cross-sectional areas were generated from a log-normal distribution [$N(\overline{x},\sigma^2)$], with mean $\overline{x} = 0$ dB and standard deviation $\sigma = 3$ dB.

At each frequency, echoes were rejected as being multiples if the standard deviation in phase samples (P_{dev}), recorded within 6 dB of the peak, exceeded a preset limit in either the athwartship or alongship directions (Bodholt, 1990). Consistent with the minimum echo length filter, echoes were also rejected if the trough in a multi-peak echo was more than 6 dB below the peak. Runs of 1000 pings were repeated at P_{dev} limits corresponding to off-axis angles of 0.1, 0.2, 0.3, 0.4, 0.5, 0.6, 0.8, and 1.0 degrees.

The echoes which passed these filters at a single-frequency were then subjected to two-frequency spatial matching criteria; echoes were rejected if (1) the range estimates at the two frequencies were not matched to within 0.1 m; and (2) the absolute difference between the respective estimates of off-axis angles (α and β) were not matched to within a specified angle discrepancy.

In some cases, unresolvable targets are falsely identified as individual scatterers by a split-beam system utilizing a single-frequency multiple-target rejection algorithm (see Sec. D of the Introduction). The deleterious nature of this problem has been clearly demonstrated [Fig. 1(a)]. Simulations of the one-frequency multiple-target rejection algorithm show a dramatic increase in the number of unresolv-

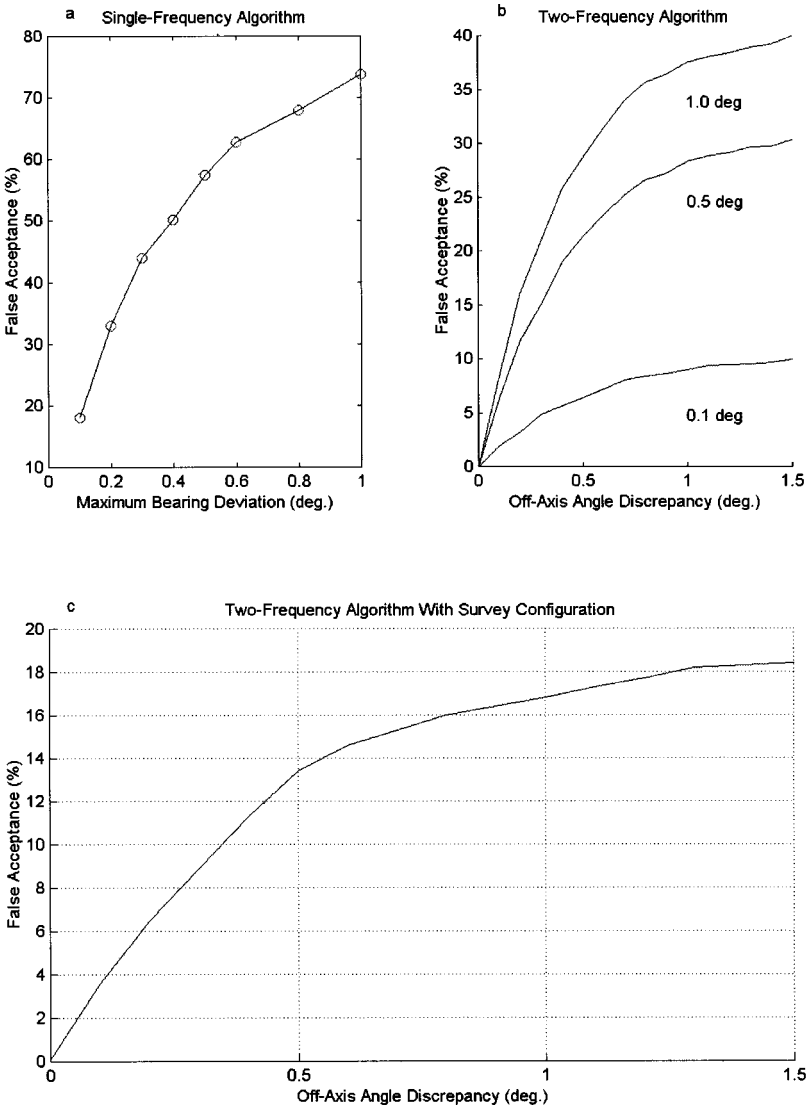

FIG. 1. Simulated false detection rates (acceptance of unresolvable scatterers as individuals) using the one- and two-frequency multiple-target rejection algorithms. With a single frequency (38 or 120 kHz), the percent of false detections rises sharply with an increase in maximum bearing deviation (electrical phase deviation converted to off-axis angles). At the default phase deviation of four steps (equivalent to a bearing deviation $A_{\mathrm{dev}} \cong 0.52$ degrees for the Simrad ES120-7 120-kHz transducer), the simulation predicts a false acceptance of about 57.9%. Using the two-frequency method (b), the false acceptance rate is dramatically reduced, even broad limits on the off-axis angle discrepancy, to less than 40%, 30%, and 10% with A_{dev} at 1.0, 0.5, and 0.1 degrees, respectively. Under the survey equipment configuration (notably, pulse lengths of 1.0 and 0.3 ms at 38 and 120 kHz, respectively), using default EK500 filter parameters (notably $A_{\mathrm{dev}} \cong 0.52$ degrees, 75.4% of the multiple targets were falsely accepted at 38 kHz, 25.3% at 120 kHz. However, using the two-frequency method (range and angle-discrepancy criteria of 0.1 to 1.5 degrees, respectively), the simulation predicts false acceptances of only 3.6 % to 18.4 % using (c). Note the scale changes.

able targets accepted with an increase in maximum bearing deviation criteria [electrical phase deviation (P_{dev}) converted to off-axis angle deviation (A_{dev})]. Using the EK500 default phase deviation setting (Table II, $P_{\mathrm{dev}}=4$ steps or $A_{\mathrm{dev}} \cong 0.52$ degrees for the Simrad ES120-7 120-kHz transducer), about 57.9% of the unresolvable multiple targets were categorized as individual scatterers. On the other hand, due to the virtual elimination of scattering interference events, the two-frequency method (as defined in the preceding paragraph) greatly reduces the false acceptances to less than 30%, even when using broad limits on the discrepancy in off-axis angles as measured with the two frequencies [Fig. 1(b)].

In order to more closely match a typical EK500 survey configuration, the simulation was repeated with pulse lengths of 1.0 and 0.3 ms, quadrant separations of 79 and 42 mm, and angle sensitivities of 12.5 and 21, at 38 and 120 kHz, respectively, and runs of 1000 pings were evaluated at the default P_{dev} limits of four phase steps ($\alpha=\beta=0.92$ at 38 kHz and 0.52 degrees at 120 kHz. Under this common configuration, 75.4% of the multiple targets were falsely accepted at 38 kHz, 25.3% at 120 kHz and only 3.6% to 18.4% using the two-frequency method with angle-discrepancy criteria of 0.1 to 1.5 degrees, respectively [Fig. 1(c)].

In short, these simulations predict that the two-frequency method for rejecting unresolvable targets will provide a performance gain of at least fourfold over the single-frequency algorithm (Note that some of the performance gains are made through a reduction in pulse length at 120 kHz.) However, in order to effectively match a target in range and off-axis angles at two frequencies simultaneously, the positional information must be precise. Exactly how precise must be answered by the requirements of the investigation and is dependent upon the SNR (Table I).

To investigate this consideration, noise measurements were recorded under actual survey conditions while conducting a survey off the South Shetland Islands, Antarctica. The 38-, 120-, and 200-kHz transducers (Simrad ES38-12, ES120-7 and ES200-28) were hull-mounted in a steel blister at a depth of about 7 m, about 30 m aft-of-bow on the 105-m-long vessel (R/V YUZHMORGEOLOGIYA). Background noise power levels (P_n) were recorded by the three EK500 receivers, operating in passive mode, with sea conditions at Beaufort 5 while surveying at a ship speed of 10 kn.

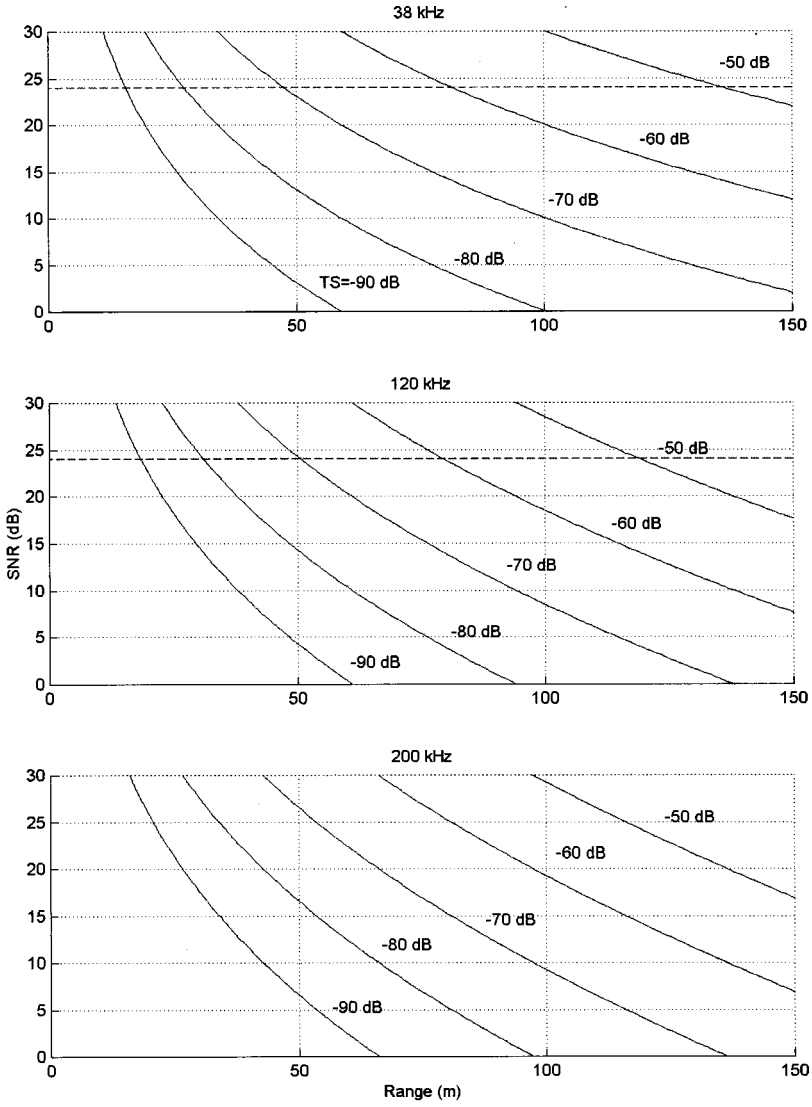

FIG. 2. Signal-to-noise ratio versus range for various TS values (solid curves). At the respective frequencies of 38, 120, and 200 kHz, the absorption coefficients (γ) were 0.01, 0.038, and 0.053 dB/m; the on-axis system gains (G) were 22.8, 24.7, and 28.0 dB; the wavelengths were 0.0382, 0.0121, and 0.0073 m; the noise powers (P_n) were measured to be -136.8, -147.0, and -148.6 dB *re*: 1 W; the pulse lengths (τ) were 1.0, 1.0, and 0.6 ms; and the transmit powers (P_t) were all 30 dB *re*: 1 W. For the EK500 echosounder operating with these conditions and parameters, maximum precision of the phase measurement is possible at a SNR of more than 24 dB (dashed line).

Under these survey conditions, the background power levels were $P_n = -136.8 \pm 0.3$ dB, -147.0 ± 0.3 dB, and -148.6 ± 0.1 dB *re*: 1 W, at 38, 120, and 200 kHz. Using these values of noise power and solving Eq. (6) for received power, the SNR was plotted versus range for various TS values (Fig. 2). Calculated from (15) and also plotted in Fig. 2 is the requisite SNR to potentially measure off-axis angles with the EK500 split-beam system to within one phase step (SNR$>$24 dB). Fortunately, Fig. 2 indicates that the maximum angular precision of the EK500 is not noise limited under typical survey conditions. However, the maximum range for this angular precision is strongly dependent upon the scattering strength of the target [Eq. (6)]. For example, considering only the constraints of noise, the off-axis angles of a euphausiid (TS~ -70 dB at 120 kHz) can be measured with maximal precision out to a range of about 50 m.

II. TANK EXPERIMENTS

Controlled experiments were conducted in a large test tank at the Institute of Maritime Technology in Simonstown, South Africa from 18 June to 26 July 1996. The tank (approximately 20 m long by 10 m wide by 10 m deep), contained fresh water at a temperature of 18 °C. An EK500 echosounder (firmware version 5.2) was configured with 38- and 120-kHz split-beam transducers (Table III). The transducers were mounted next to each other, 4 m deep and 6 m from one end of the tank, so as to project horizontally down the length of the tank.

A. TS measurement precision

1. On-axis measurements

In order to utilize the multi-frequency method for *in situ* TS measurements, it was first necessary to characterize the

TABLE III. Echosounder and transducer specifications (nominal).

Simrad EK500 (kHz)	38	120	200
Frequency (kHz)	37.878	119.047	200.000
Transducer model	ES38.12	ES120-7	ES200-28E
3 dB beamwidth (degrees)	12 ± 1	7.1	7.0 ± 1
Angle sensitivity (Λ)	12.5	21.0	[a]
Angular resolution (ζ) (degrees)	0.225	0.134	[a]
Range cell (m)	0.10	0.03	0.02
Pulse duration (τ) (ms)	1.0	0.3	0.6
Receiver bandwidth (kHz)	3.8	12.0	2.0

[a]Not applicable for single-beam transducer.

TABLE IV. Nominal on-axis TS measurements of standard spheres at 38 and 120 kHz in fresh water at a temperature of 18.9 °C. Also shown are (1) the differences in TS at these two frequencies; (2) the ratio of these differences to the sphere diameters; and (3) the slope of TS versus the logarithm of the product of the wave number and the spherical radius (a). All measurements were made with the same system gain settings. The TS measurements typically ranged at least ±0.5 dB (see Fig. 2).

Sphere diameter ($2a$)	23 mm Cu	30.05 mm Cu	38.1 mm WC	60 mm Cu
$TS_{120\ kHz}$ (dB)	−40.4	−36.3	−39.3	−33.3
$TS_{38\ kHz}$ (dB)	−48.0	−40.5	−42.3	−33.1
$TS_{120}-TS_{38\ kHz}$ (dB)	7.6	4.2	3.0	−0.2
$(TS_{120}-TS_{38\ kHz})$/Diameter (dB/m)	330.4	139.8	78.7	−3.3
$ka_{120\ kHz}$	5.8	7.6	9.6	15.1
$ka_{38\ kHz}$	1.8	2.4	3.0	4.8
Slope of TS vs Log(ka)	55.7	44.8	45.4	33.0

measurement precision of the split-beam system. First, TS measurements were made at both frequencies of four standard spheres [23.0, 30.05, and 60 mm copper (Cu), and 38.1 mm diameter tungsten carbide with 6% cobalt binder (WC)] (Table IV). In succession, each standard sphere was placed on the beam-axis approximately 10 m from the transducer. The spheres (Foote, 1983, 1990) were suspended by a monofilament line which was attached to the WC sphere by a monofilament knotted bag, and to each Cu sphere by a loop of monofilament nylon affixed into a single shallow bore.

At both 38 and 120 kHz, TS measurements of the four spheres exhibited variances typically greater than 0.5 dB (Table IV). For the three largest spheres, the differences in TS (120–38 kHz) decreased linearly versus increasing sphere diameter. For the 23-mm Cu sphere, which is approximately 60% smaller than the wavelength at 38 kHz (ap-

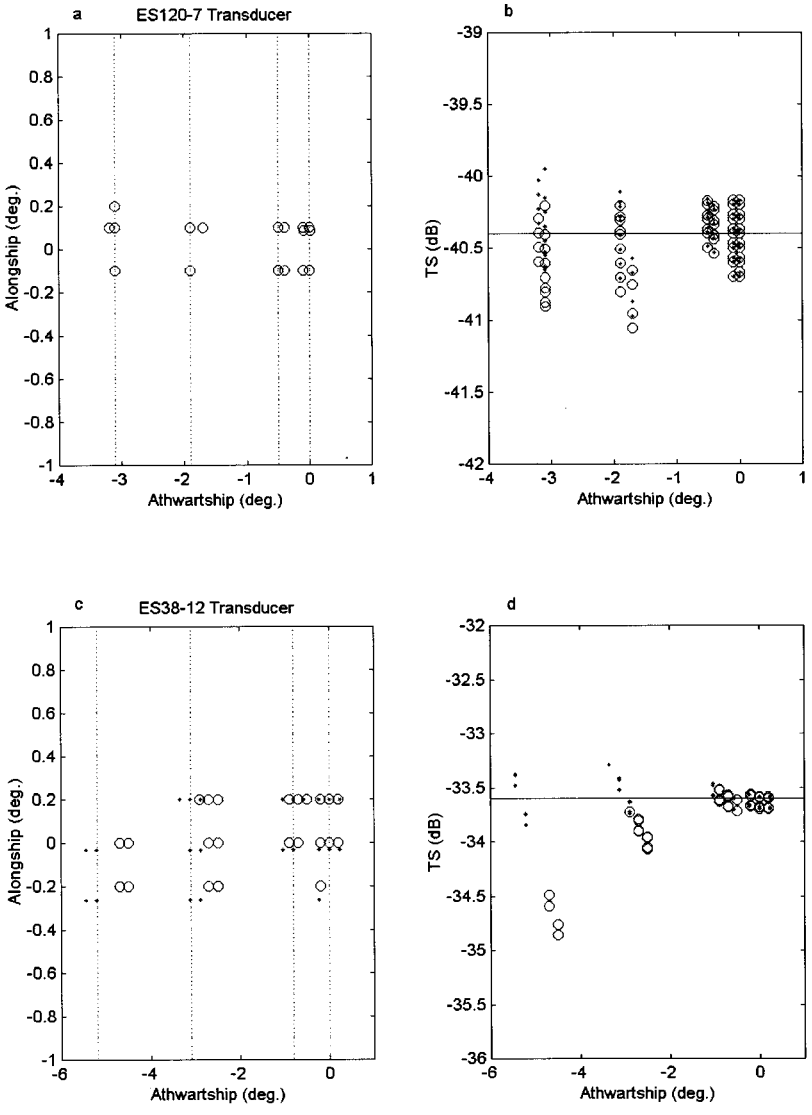

FIG. 3. Measurement of transducer angle sensitivity. For the ES120-7 transducer [(a) and (b)], a 23-mm Cu sphere was positioned at a range of 10.0 m and off-axis distances of 0, 87, 325, and 537 mm (0.0, −0.5, −1.9, and −3.1 degrees). From these TS measurements (○), the nominal value for this transducer ($\Lambda=21.0$) was shown to differ from value judged optimal ($\Lambda=20.5$, obtained by detrending the TS data with respect to off-axis angle) to within the angular resolution (≅0.134 degrees). The measurements were repeated (○) for the ES38-12 transducer [(c) and (d)] using a 60 mm Cu sphere at a range of 10.0 m and off-axis distances of 0, 147, 550, and 909 mm (0.0, −0.8, −3.1, and −5.2 degrees). The nominal value for this transducer ($\Lambda=12.5$) was shown to differ greatly from the value judged optimal ($\Lambda\cong10.8$). The lesser angular resolution at 38 kHz (≅0.225°) results in greater measurement variability. At both frequencies, the corrected angle sensitivity reduced the bias in off-axis TS measurements (•).

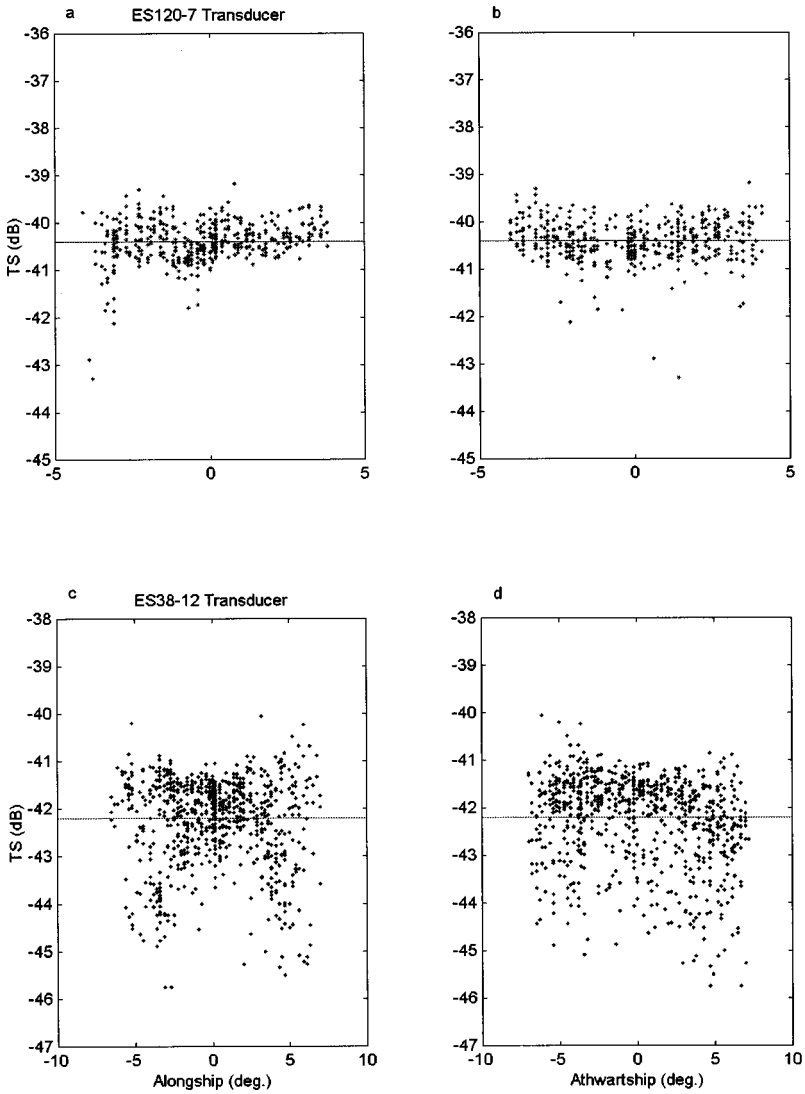

FIG. 4. Precision of TS measurements versus off-axis angle. In the test tank, the TS of a 23 mm Cu sphere was measured as it was moved, at a range of 10 m, through the beams of the ES120-7 transducer. Likewise, the TS of a 38.1 mm WC sphere was measured with the ES38-12 transducer. Plotted are the measured (•) and theoretical TS values (–).

prox. 39 mm), the TS difference versus the sphere diameter is more than three times greater than that for the others.

2. Off-axis measurements

The precision of off-axis measurements is primarily related to the accuracy of Λ, $B(\alpha,\beta)$ and ζ, and the SNR. The nominal angle sensitivity for the 120-kHz transducer was measured next by placing a 23-mm Cu sphere 10.0 m from the transducer and off-axis by distances of 0, 87, 325, and 537 mm (0.0, −0.5, −1.9, and −3.1 degrees). The measurements were repeated for the 38-kHz transducer using a 60-mm Cu sphere at a range of 10.0 m and off-axis distances of 0, 147, 550, and 909 mm (0.0, −0.8, −3.1, and −5.2 degrees) (Fig. 3).

For the ES120-7 transducer, the measured value for Λ (20.5) differed from the nominal value (21.0). For the ES38-12 transducer, the difference was much greater (measured $\Lambda \cong 10.8$ versus nominal $\Lambda = 12.5$). At both frequencies, the corrected angle sensitivity reduced the bias in off-axis TS measurements (Fig. 3). Note also that the decreased angular resolution at 38 kHz ($\cong$0.225 degrees) results in significantly greater measurement variability.

Using the measured angle sensitivities, the general precision of individual TS measurements was characterized by moving an individual sphere within the confines of the transducer 3-dB beamwidth. The TS values were recorded versus off-axis angles at 38 kHz using the 38.1-mm WC sphere and at 120 kHz using the 23-mm Cu sphere (Fig. 4).

As a 23-mm Cu sphere was moved through the beam of the ES120-7 transducer at a range of 10 m, the TS measured at 120 kHz ranged 4.1 dB (σ=0.4 dB) [Fig. 4(a) and (b)]. Similarly, while moving a 38.1-mm WC sphere through the beam of the ES38-12 transducer at 10-m range, the TS measurements ranged 5.7 dB (σ=1.0 dB). At 38 kHz, the decreased measurement precision is due to the lower range and angular resolutions, coupled with a possible mismatch between modeled and actual beam-patterns [Fig. 4(c) and (d)].

B. Multiple target rejection

1. Single-frequency algorithm

The effectiveness of the EK500 algorithm for rejecting multiple targets was evaluated for a benchmark by moving two spheres randomly within the same resolution volume (Fig. 5). At 38 kHz, the TS detections were recorded while two 60-mm Cu spheres (each nominal TS=−33.6 dB) were

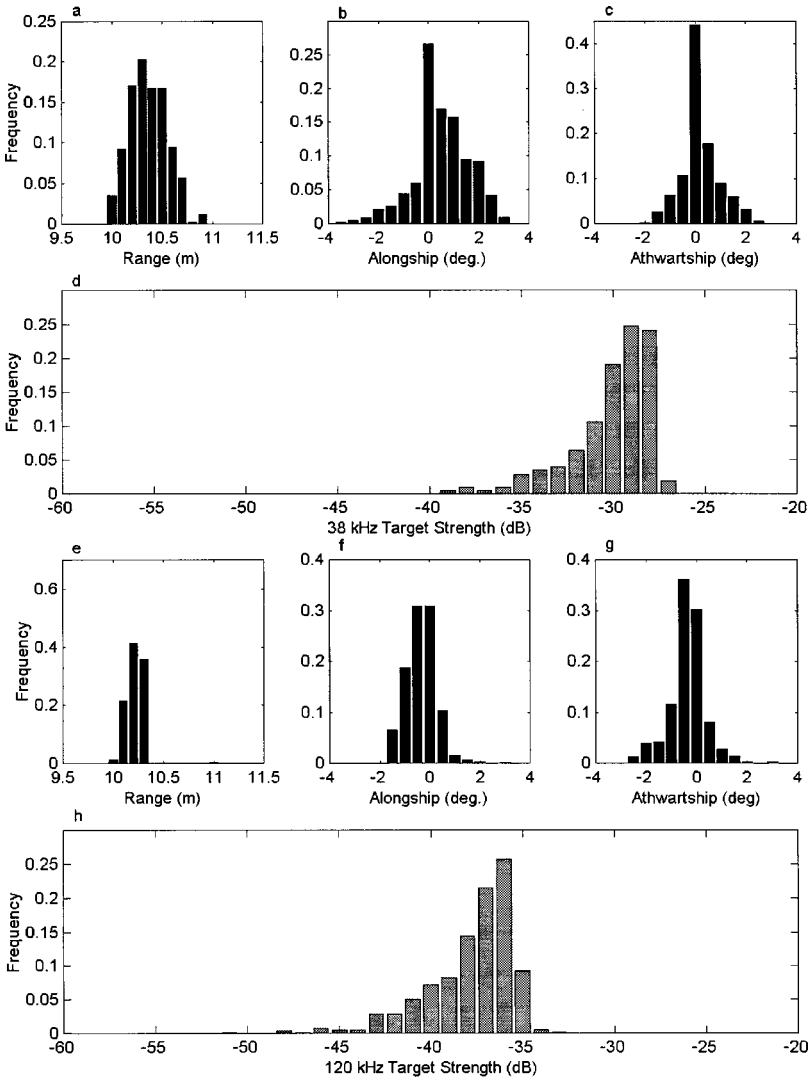

FIG. 5. Single target detections at 38 and 120 kHz from a field of two spheres. At 38 kHz [(a)–(d)], two 60-mm Cu spheres (each −33.6 dB; Foote, 1983) were moved randomly ±2.17 degrees off-axis (±0.380 m) and within a single range resolution volume (10 to 10.75 m). At 120 kHz [(e)–(h)], two 23-mm Cu spheres (each −40.4 dB) were moved randomly ±2.17 degrees off-axis (±0.380 m) and within a single range resolution volume (10 to 10.225 m).

randomly moved ±2.17 degrees off-axis (±0.380 m) and in range from 10 to 10.75 m. At 120 kHz, two 23-mm Cu spheres (each nominally −40.4 dB) were randomly moved ±2.17 degrees off-axis (±0.380 m) and in range from 10 to 10.225 m.

At 38 kHz, the EK500 falsely misinterpreted two acoustically unresolvable 60.0-mm Cu spheres (TS=−33.6 dB; Foote, 1983) as individuals in 35% of the 1200 pings (Fig. 5). Resulting from interference effects, the TS distribution is shifted upward (mean=−29.6 dB), ranges 12.2 dB (σ=2.2 dB), and has minimum values as low as −39.1 dB. Similarly at 120 kHz, the two 23.0 mm Cu targets (TS=−40.4 dB) were falsely misinterpreted as individuals in 40% of the 1500 pings. The distribution of measurements is negatively skewed (mean=−37.3 dB), ranges 27 dB (σ=2.5 dB), and has minimum values as low as −60 dB.

2. Multiple-frequency method

The effectiveness of matching TS detections at multiple frequencies for rejecting unresolvable echoes was then investigated. First it was necessary to derive tolerances for matching target positions at two or more frequencies. To do so, measurements of a single 23-mm Cu sphere (range, off-axis angle, and TS) were made simultaneously at 38 and 120 kHz. At a nominal range of 10 m, the sphere was moved horizontally and randomly inside the confines of a box 1.1 by 0.76 m (Fig. 6).

With the two transducers mounted adjacently (Fig. 7),

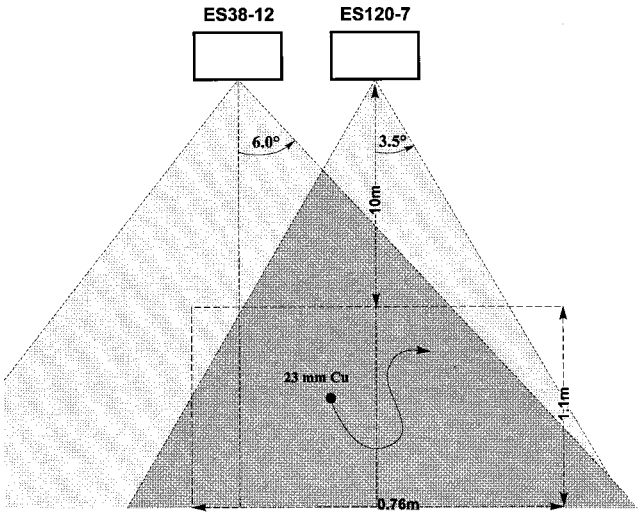

FIG. 6. Simultaneous TS measurements of a 23-mm Cu sphere at 38 and 120 kHz. At a nominal range of 10 m, the sphere was moved randomly inside the confines of a box 1.1 by 0.76 m^2. The drawing is not to scale.

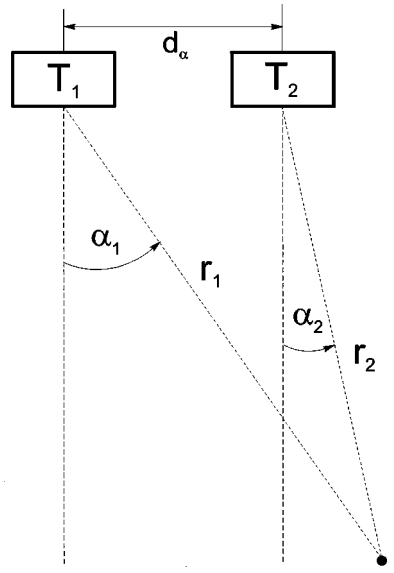

FIG. 7. Matching target detections from two adjacent transducers. The off-axis angles (α_1 and α_2) and the slant ranges (r_1 and r_2) are interrelated by the separation of the parallel transducer axes (d_α).

beam axes parallel, α, β, and r are related by the separation of the beam axes in the alongship and athwartship planes (d_α, d_β):

$$\alpha_2 = \sin^{-1}\left(\frac{r_1 \sin\alpha_1 - d_\alpha}{r_2}\right)$$

and (17)

$$\beta_2 = \sin^{-1}\left(\frac{r_1 \sin\beta_1 - d_\beta}{r_2}\right).$$

The angular discrepancy between the two systems [theoretical α_{120} or β_{120} (calculated from $d_{38\text{-}120}$ and α_{38} or β_{38}) minus measured α_{120} or β_{120}, respectively] was ± 1.5 degrees (>95% confidence). This can be attributed to a combination of (1) the angular resolutions of the two systems; (2) some unknown rotational angles inherent in the transducer mounting or beam-pattern; (3) noise; and (4) the polychromatic transfer functions or scattering complexity of the individual scatterers.

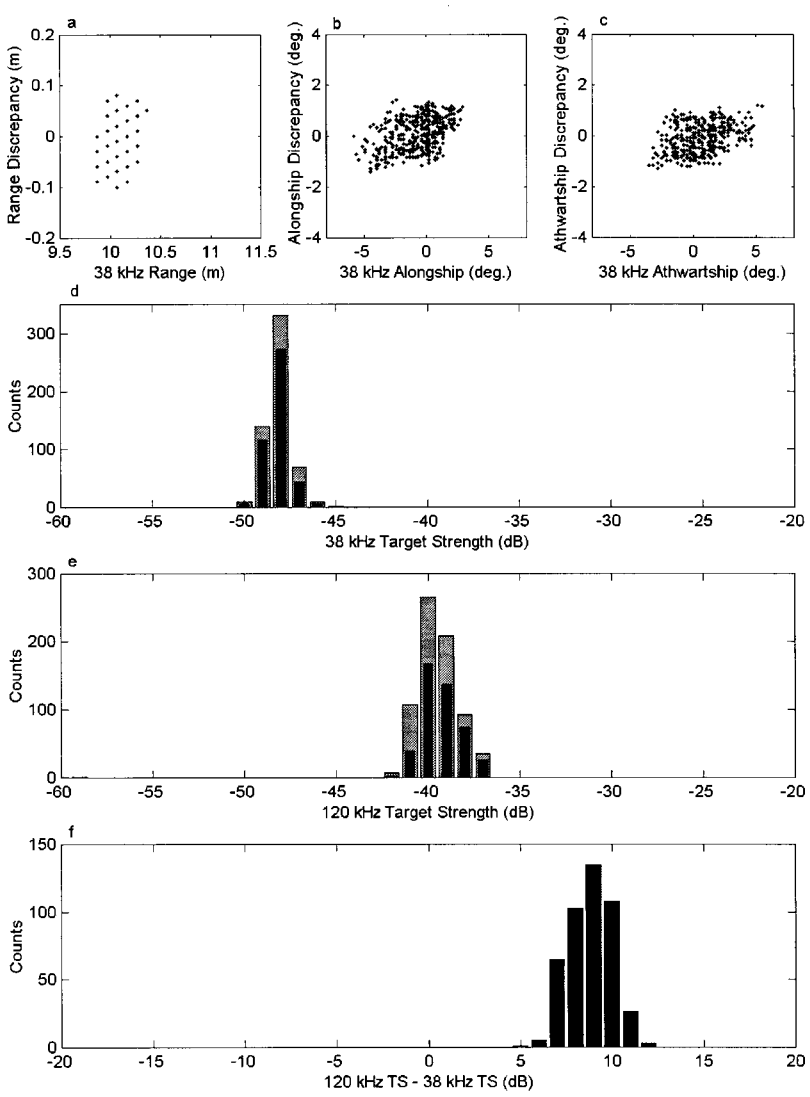

FIG. 8. The TS measurements of a single 23.0-mm Cu sphere at a range of 10 m, moved randomly through the beams of juxtaposed 38 and 120 kHz transducers. From 1000 pings, the single-frequency algorithm accepted 560 and 717 measurements at 38 and 120 kHz, respectively (gray bars). Of these, the two-frequency method accepted 440 measurements; a reduction of 21% to 39% (black bars).

Due to the differing bandwidths and sampling rates of the two systems and a small offset of the two transducer faces, target ranges at 38 kHz (r_{38}) were consistently about one sample range ($\cong$0.1 m) greater than the more accurate range estimates (r_{120}) of the 120-kHz system (sample range $\cong$0.03 m) and both ranges were slightly greater than the actual ranges. In order to compensate for the receiver delay, measurements of target ranges were reduced by three sample ranges or by 0.3 m at 38 kHz and 0.09 m at 120 kHz and then a residual mean offset of 0.07 m was subtracted from the 38-kHz ranges (Figs. 8, 10, and 12). After applying these corrections, the variation in range discrepancy [theoretical r_{120} (calculated from $d_{38\text{-}120}$ and measured r_{38}) minus measured r_{120}] for a single 23-mm Cu sphere was $\pm$0.1 m (>95% confidence). (Note, the EK500 firmware V5.2 and V5.3 subtracts three sample ranges and interpolates between range cells for the purpose of transmission loss compensation only—not range).

The tolerances for spatial matching were then used in the multi-frequency method for rejecting multiple targets. Specifically, targets were only accepted as individual scatterers if the single-target detections at each frequency were matched to within $\pm$1 range cell at 38 kHz (0.1 m) and to an off-axis angular discrepancy of 1.5 degrees. The target ranges could be matched this closely because the filter averaging times ($\cong$1/bandwidth), in terms of range cells, are very small and virtually identical at both frequencies (1/3.8 kHz=0.263 ms/133 μs/sample=1.9725 samples at 38 kHz and 1/12.0 kHz=0.08 ms/40 μs/sample=2 samples at 120 kHz). For a single 23-mm Cu sphere moved randomly inside the two partially overlapping beams, single-target detections with the single-frequency algorithm totaled 560 and 717 out of 1000 pings at 38 and 120 kHz, respectively (Fig. 8). In contrast, the two-frequency method accepted only 440 measurements or 21% to 39% fewer than the single-frequency method with no bias or change in variance (Fig. 8).

For both the single- and multiple-frequency algorithms, the ranges of TS measurements were greater than 5 dB. It is also important to note that the variance in TS differences [var $(TS_{120}-TS_{38})$] is worse than either of the single-frequency measurements due to the compounding of measurement errors; it is expected to be the sum of the variances of the single-frequency measurements plus twice the covariance (Rice, 1988).

The TS measurements were also made of three spheres residing within 1.47 and 4.89 range cells at 38 and 120 kHz, respectively (Fig. 9). The 23-mm Cu sphere was fixed into position on the beam axis of the 120-kHz transducer at a range of 10 m while a 30.05-mm Cu and a 38.1-mm WC sphere were moved randomly inside the confines of the 1.1 by 0.76 m box. Two-frequency TS measurements were again recorded.

Theoretically, a single target could be accurately detected in this configuration, but the probability of a single sphere residing within one 38-kHz resolution volume is low (0.175 to 0.225 with 95% confidence from Monte Carlo simulation of 1000 runs of 1000 pings) and delineation of more than one sphere per ping is physically impossible. Nonetheless, out of 1000 pings, detections with the single-frequency algorithm totaled 329 at 38 kHz and 1059 at 120 kHz (some multiple detections per ping).

Applying the two-frequency method, 89% and 96% of the single-frequency detections were rejected as multiple-scatterers at 38 and 120 kHz, respectively (Fig. 10). Of the remaining 38 TS measurements, there was no more than one target detection in any single ping. The histogram of TS differences exhibits a main peak corresponding to the 30.05-mm Cu sphere and the 38.1 mm WC sphere and a smaller peak corresponding to the 23-mm Cu sphere. Additionally there are two small peaks at plus and minus 1 dB, probably due to a residual of multiple targets accepted [0.6% (38 kHz) to 1.8% (120 kHz) of single-frequency detections] with the Version 5.2 default detection criteria (Table II).

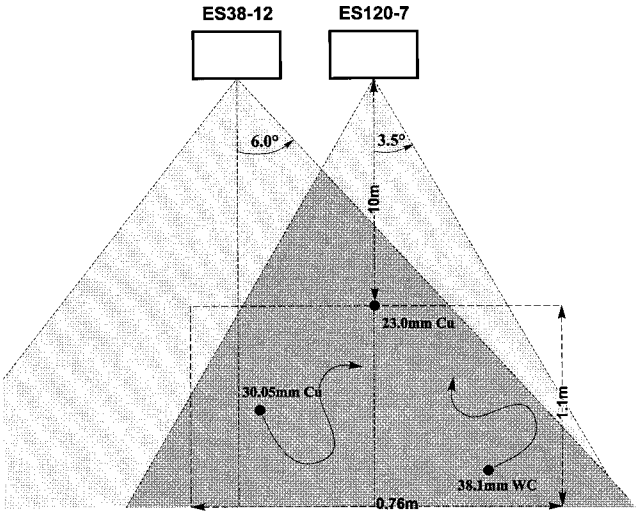

FIG. 9. Simultaneous TS measurements of a 23-mm Cu sphere were made at 38 and 120 kHz while a 30.05-mm Cu and a 38.1-mm WC sphere were moved randomly inside the confines of a box 1.1 by 0.76 m^2. The drawing is not to scale.

III. FIELD EXPERIMENTS

In situ target strength measurements were collected off the western side of the Antarctic Peninsula from mid-January through mid-February 1997. The shipboard echosounder system (Simrad EK500; firmware version 5.2) was configured with 38- and 120-2 kHz split-beam transducers (different than those used in the tank experiments, but the same models) and a 200-kHz single-beam transducer (Table III). The down-looking transducers were mounted on the hull of the ship, in a row (from fore-to-aft: ES120-7, ES38-12, ES200-28), approximately 7 m deep. The system was calibrated using a 38.1-mm WC sphere (Foote, 1990), before and after the survey at Ezcura Inlet, King George Island. Acoustic transects were conducted for 14 consecutive days in an area around Elephant Island (AMLR, 1997). Approximately every 30 km, acoustic targets were sampled with a 2.5-m^2 Isaacs-Kidd midwater trawl (IKMT) fitted with a 505-μm mesh net (Devereaux, 1953).

A total of 105 IKMT tows were conducted concurrently with collections of acoustic target strength. From the samples, 73 zooplankton and nekton species and categories

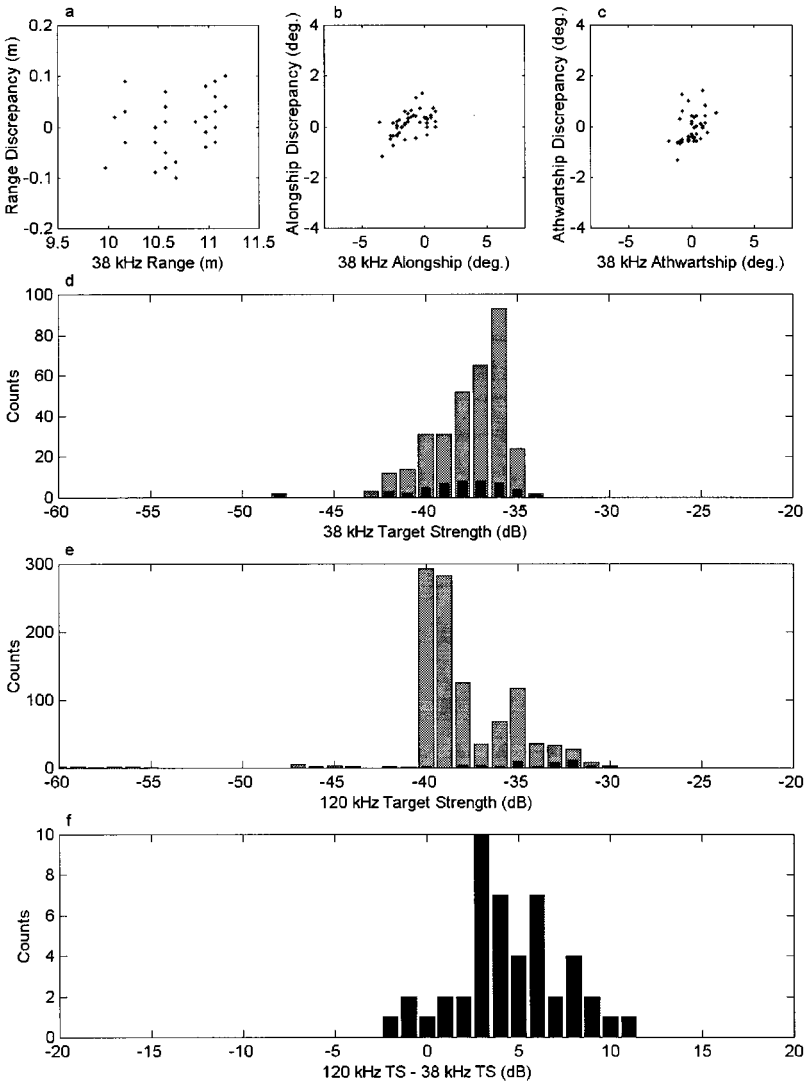

FIG. 10. Testing the two-frequency method for multiple target rejection. A 23-mm Cu sphere was positioned on the axis of the 120-kHz transducer at a range of 10 m while two other spheres (30.05 mm Cu and 38.1 mm WC) were randomly moved around the sphere within 1.47 and 4.89 range cells at 38 and 120 kHz, respectively. The probability of accurately detecting an individual scatterer in this proximity is very low. From 1000 pings, detections with the single-frequency algorithm totaled 329 at 38 kHz and 1059 at 120 kHz (gray bars). In sharp contrast, the two-frequency method passed only 38 measurements, rejecting 89% to 96% as multiple-scatterers (black bars).

were identified, including crustacean invertebrates, gelatinous tunicates, chaetognaths, and myctophid fishes. The four most numerically abundant taxa, caught in over 90% of the tows, were (1) copepods; (2) a pelagic tunicate (*Salpa thompsoni*, with length modes of individual animals at 10, 25, and 45 mm); (3) two euphausiids [*Thysanoessa macrura*, less than 20 mm mean length and *Euphausia superba* (Antarctic krill) with length modes at 26, 37, and 50 mm]; and (4) an amphipod (*Themisto gaudichaudii*, less than 10 mm mean length). The taxa with the largest animals included euphausiids (*T. macrura* and *E. superba*), and two species of myctophids (*Electrona carlsbergi*, range 70–90 mm; and *Electrona antarctica*, range 40–110 mm). The myctophids were caught in approximately 10% of the tows, although their distribution appeared to be much more widespread from an examination of the echograms. Their under-representation in the IKMT catches may be explained by the ability of these fish to avoid the relatively small net.

Before the multi-frequency method could be applied to the field measurements of *in situ* TS, the minimum detection ranges were determined. For simultaneous detections at two (38 and 120 kHz) and three frequencies (38, 120, and 200 kHz), the minimum ranges ($r\min_{38\text{-}120}$ and $r\min_{200\text{-}120}$) are functions of the transducer separations ($d_{38\text{-}120}$ and $d_{200\text{-}120}$) and the maximum allowable off-axis angles for each transducer ($\phi_{38}, \phi_{120}, \phi_{200}$):

$$r\min_{38\text{-}120} = \left(\frac{d_{38\text{-}120}/\tan(\phi_{38})}{1 + (\tan(\phi_{120})/\tan(\phi_{38}))} \right)$$

and (18)

$$r\min_{200\text{-}120} = \left(\frac{d_{200\text{-}120}/\tan(\phi_{200})}{1 + (\tan(\phi_{120})/\tan(\phi_{200}))} \right).$$

For the shipboard transducer mounting configuration (Fig. 11; $d_{120\text{-}38} = 0.4425$ m and $d_{38\text{-}200} = 0.4425$ m, and targets accepted within the 3-dB beamwidths ($2\phi_{38} \cong 12$ degrees, $2\phi_{120} \cong 2\phi_{200} \cong 7$ degrees), $r\min_{38\text{-}120} = 2.7$ m and $r\min_{200\text{-}120} = 7.2$ m.

When moving from a test tank to the field, the measurements of range and off-axis angle may be affected by increases in the number of noise sources and target complexity. However, if the condition of far-field operation is imposed (with respect to the apertures of both the transducer and the targets), the receiver bandpass filters (Table III) could be expected to reduce the measurement uncertainty due to noise and the complex nature of real scatterers. Therefore, consistent with the tank experiments, the single-target

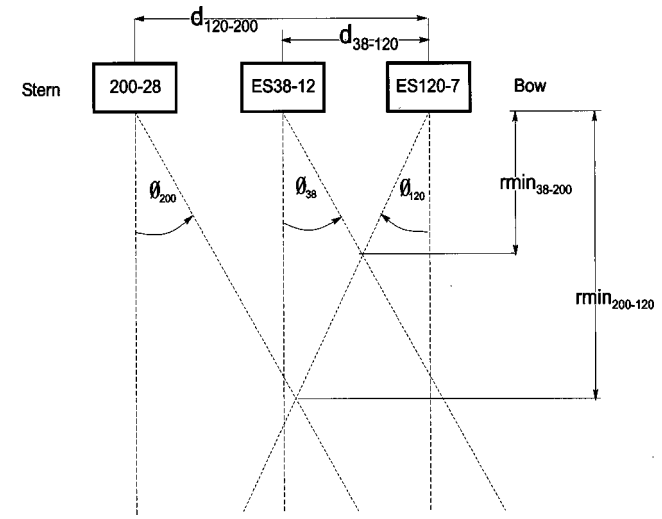

FIG. 11. Minimum ranges for TS matches using multiple transducers. The minimum ranges for simultaneous detections at two- and three-frequency systems ($r\min_{38\text{-}120}$ and $r\min_{200\text{-}120}$) are functions of the maximum allowable off-axis angles (ϕ) and the horizontal separations between beam axes ($d_{38\text{-}120}$ and $d_{200\text{-}120}$, respectively).

detections at 38 and 120 kHz were matched to within ±1 range cell at 38 kHz (0.1 m) and constrained to an off-axis angular discrepancy of 1.5 degrees. Once again, 82% to 96% of the single-frequency single-target detections were rejected as multiple targets (Fig. 12).

The *in situ* TS measurements were plotted versus range for one-frequency [Fig. 13(a) and (b)] and two-frequency detections [Fig. 13(c) and (d)]. With the two-frequency method, a large proportion of the unresolvable targets were rejected at large ranges. This was expected because the insonified volumes increase with increasing range, and the probabilities of resolving individual animals decreases accordingly. Of note, however, is the preferential rejection of smaller targets as described by the SNR required (24 dB) to measure off-axis angles to within one quantization step. Approximately 87% to 98% of the two-frequency matches were above this SNR at 38 and 120 kHz, respectively.

Corresponding TS values at 200 kHz were extracted from single-beam data by matching range bins to within ±1 range cell at 38 kHz. Consistent with the firmware implementation at the other two frequencies (Simrad, 1996), the

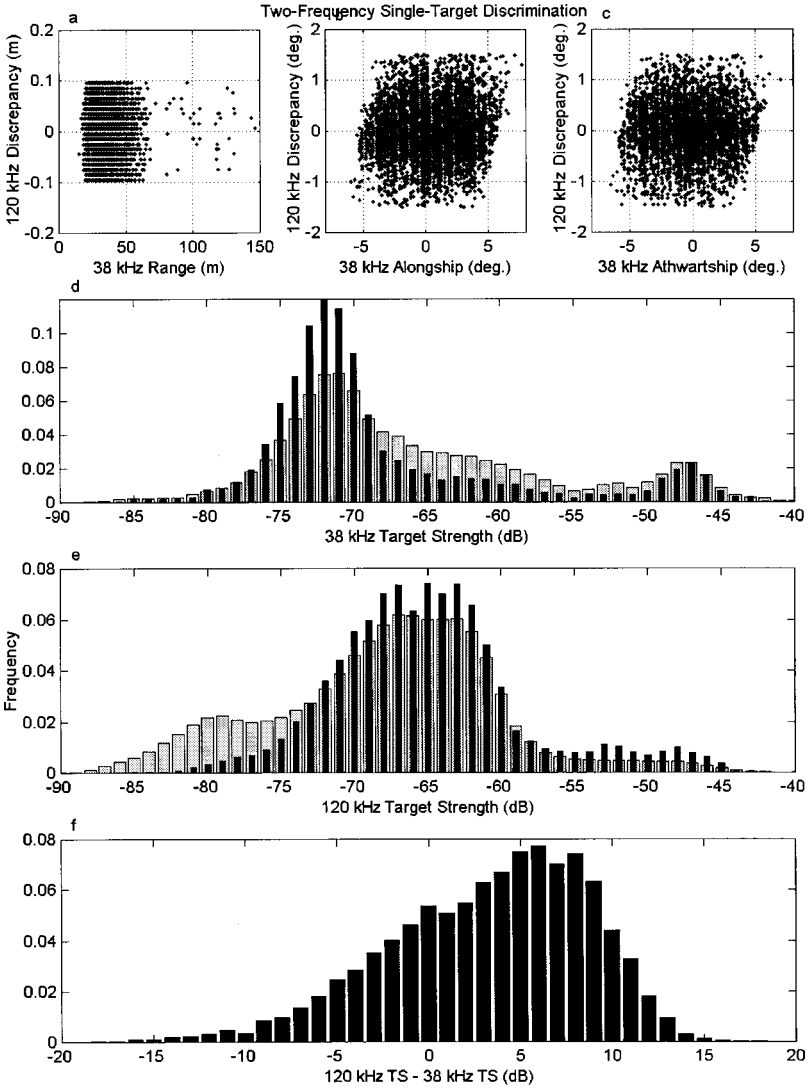

FIG. 12. *In situ* TS measurements of individual Antarctic zooplankton and nekton. Total detections using a single-frequency method (gray bars) were 40 391 at 38 kHz (d) and 173 512 at 120 kHz. (e) Using the two-frequency method, these numbers were reduced by 82% to 96% as only 7248 individual scatterers were detected (black bars).

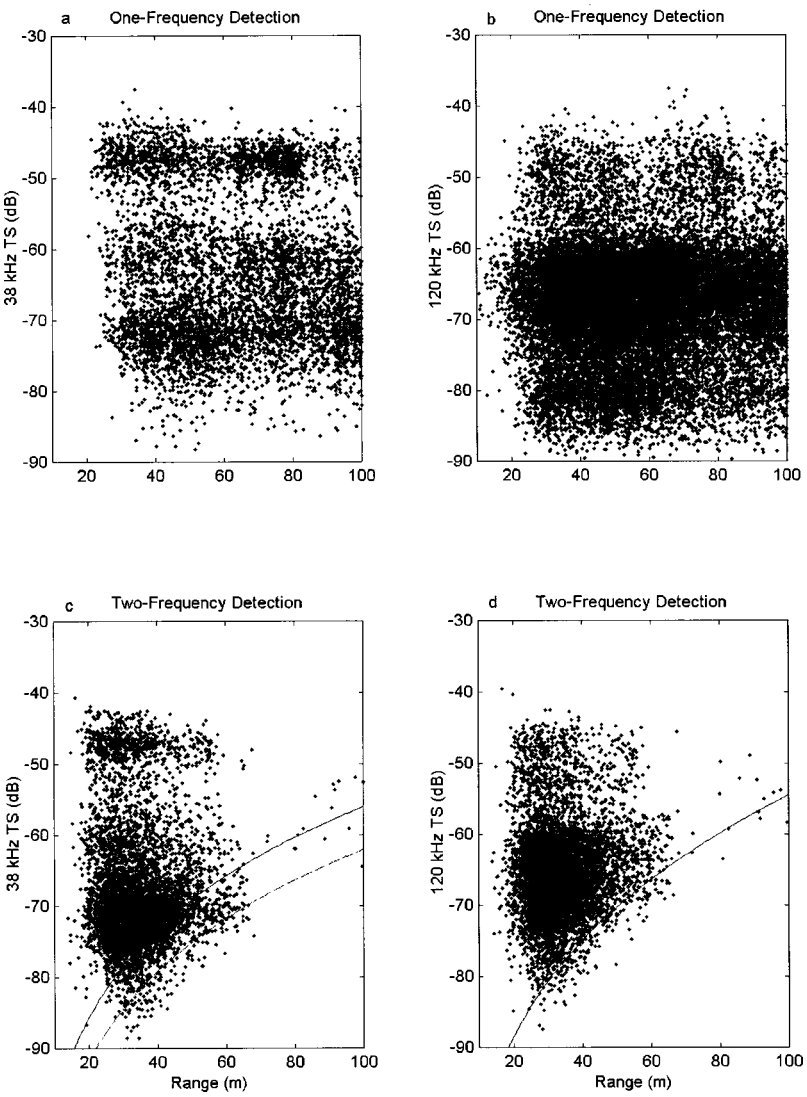

FIG. 13. Scatter plots of *in situ* TS versus range for one [(a) and (b)] and two-frequency detections [(c) and (d)]. With the two-frequency method, most unresolvable targets are rejected at large ranges where the insonified volumes are increasingly larger and the probability of resolving an individual animal is increasingly lower [(c) and (d)]. Also apparent is the rejection of smaller targets with a SNR smaller than that required (24 dB) to measure off-axis angles to within one quantization step (solid curve). At 38 and 120 kHz, 87.3% and 98.0% of the two-frequency matches were above this 95% confidence interval, respectively. At 38 kHz, 98.6% of the matches were above the SNR required (18 dB) to measure off-axis angles to within two phase quantization steps (dashed curve).

approximated one-way beam pattern $[\hat{B}(\alpha,\beta)]$ of the circularly symmetric transducer was

$$\hat{B}(\alpha,\beta) = -3\left[\left(\frac{\alpha}{\phi/2}\right)^2 + \left(\frac{\beta}{\phi/2}\right)^2 - 0.18\left(\frac{\alpha}{\phi/2}\right)^2\left(\frac{\beta}{\phi/2}\right)^2\right], \tag{19}$$

where ϕ is the 3-dB beam width of the transducer. Beampattern effects were thus removed from the resulting 200 kHz single-beam data by using the split-beam positional information of the 120-kHz transducer (Fig. 14).

As is frequently the case in fisheries acoustics, the net samples were suspected of bias (especially for nekton) and indisputable matches to the *in situ* TS measurements were impossible. Therefore, the backscattering taxa must be inferred from a combination of catch data, modes in the TS distributions, and theoretical expectations of scatterer reflectivity as a function of acoustic wavelength and animal size (Chu *et al.*, 1992).

Euphausiids were expected to exhibit Rayleigh scattering at 38 kHz and geometric scattering at 120 and 200 kHz (Demer and Martin, 1995). As such, mean TS values were expected to increase with frequency and the differences between TS measurements of euphausiids at 38 kHz and those at 120 and 200 kHz were expected to be larger and have greater variance than for animals scattering in the geometric regime at all three frequencies (e.g., fish). In the case of fish, TS was expected to decrease or increase versus frequency, depending on the existence or lack of swim-bladders, respectively (MacLennan and Simmonds, 1992).

Prior to the application of the multi-frequency method, three modes were apparent in the 120-kHz TS distribution (Figs. 12 and 13): a primary mode at about −65 dB, a secondary mode at approximately −79 dB, and a tertiary mode at about −50 dB. When selecting only those targets detected by 38 and 120 kHz, the secondary mode, possibly due to individual *S. thompsoni* or small euphausiids, was eliminated by thresholding (Foote, 1991; MacLennan and Simmonds, 1992) at 38 kHz.

After selecting only those targets which were detected simultaneously at three frequencies (Fig. 14), three modes are apparent in the 38-kHz TS distributions (Table V). Mean TS values for mode 1 were 5 to 6 dB lower at 38 kHz relative to the higher frequencies, indicating small scatterers relative to the largest wavelength (39 mm). For mode 2, the mean TS values were virtually identical, suggesting a large scatterer relative to all three wavelengths. Mode 3 averaged 3

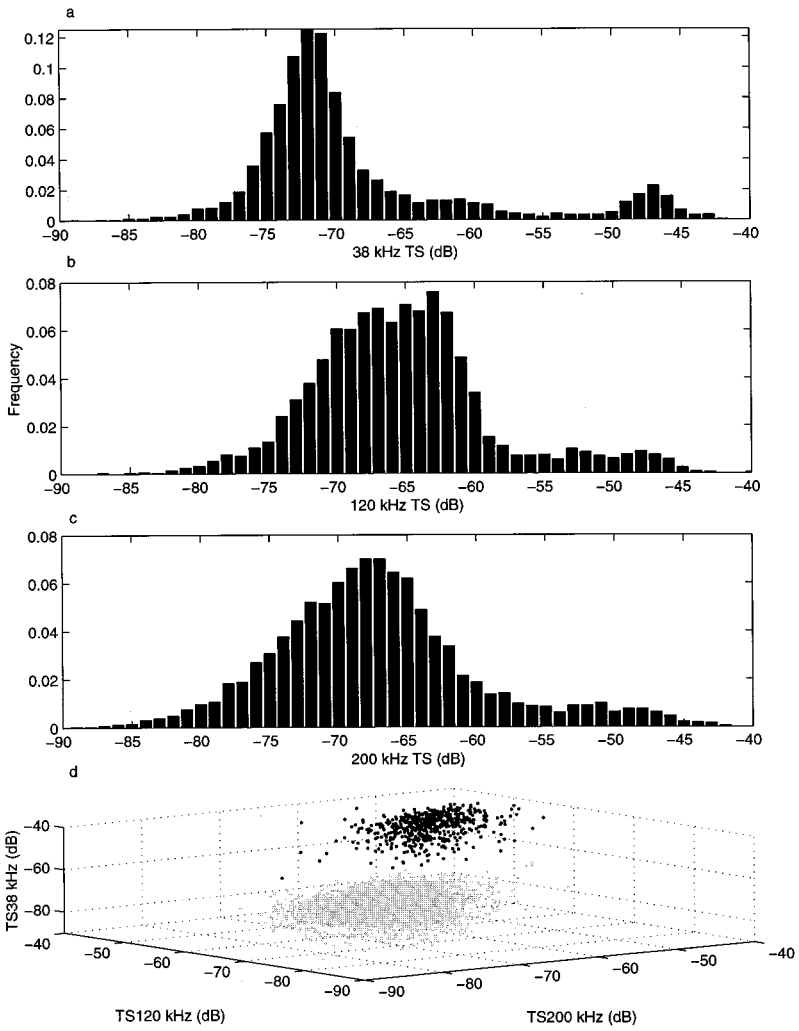

FIG. 14. *In situ* TS of Antarctic scatterers at 38, 120, and 200 kHz. Matches of single-target detections at all three frequencies totaled 5690. The 38 kHz histogram [(a)] contains three modes: $-85 \leqslant$mode $1 < -65$ dB; $-65 \leqslant$mode $2 < -55$ dB; and $-55 \leqslant$mode $3 < -40$ dB. Mode 1 (black dots) and mode 3 (gray dots) are clearly distinguishable by the three-frequency TS characterization [(d)].

dB higher TS values at 38 kHz relative to 120 and 200 kHz, possibly due to scattering from a swim-bladder. The predominant scattering species, which may be attributed to these modes, are Antarctic krill (*E. superba*) for mode 1 and *Electrona spp*. for modes 2 and 3. Improved correlations may be obtained by matching TS distributions and catch data in smaller increments of time and space.

IV. DISCUSSION

The application of echo integration methods for accurately measuring areal density of pelagic scatterers should involve simultaneous and accurate measurements of volume backscattering strength (S_v) and TS of the individual scatterers. When measuring TS *in situ*, it is necessary to eliminate measurements when multiple animals reside in the same sample volume. This constraint is particularly important when making measurements of macro zooplankton (e.g., euphausiids) or small pelagic fish (e.g., myctophids) which frequently aggregate in high density swarms and schools.

In situ TS measurements of animals at the periphery of conspecific aggregations may be more representative of animals encountered during the survey than TS distributions generated from theoretical models or controlled experiments. However, it is possible that scattering from solitary animals is not representative of that from more densely aggregated animals. Furthermore, thresholding can bias the measure-

TABLE V. *In situ* TS measurements at three frequencies. Tabulated are the means and standard deviations (σ) for three modes in the 38-kHz histogram and the same for target matches at 120 and 200 kHz. Mean TS values for mode 1 were 5 to 6 dB lower at 38 kHz relative to the higher frequencies, indicating scatterers with small backscattering areas relative to the largest wavelength (39 mm). For mode 2, the mean TS values were virtually identical, suggesting a large scatterer relative to the wavelengths. Mode 3 averaged 3 dB higher at 38 kHz relative to 120 and 200 kHz, possibly due to scattering from a swimbladder.

Frequency (kHz)	$-85 \leqslant$mode $1 < -65$ dB	$-65 \leqslant$mode $2 < -55$ dB	$-55 \leqslant$mode $3 < -40$ dB
38	−71.1 (3.1)	−60.5 (2.5)	−47.2 (2.7)
120	−65.0 (4.7)	−61.4 (4.7)	−50.0 (5.0)
200	−66.1 (5.3)	−60.2 (5.6)	−50.1 (5.4)

ments if inappropriate frequencies are chosen for the scattering taxa of interest; this is also the case for measurements of S_v.

This multi-frequency extension to the single-target detection algorithm proved very efficient at excluding unresolvable targets, relative to the single-frequency algorithm, in simulations, test tank experiments, and field studies. In one Antarctic survey, results suggest that the multi-frequency method provided a 98.2% to 99.4% improvement over the single-frequency method. There was some indication of measurement bias due to thresholding, but this can be minimized via optimal selection of frequencies for the scatterers of interest. By considering the known or expected distributions of animal size, shape, orientation, and acoustic impedance, adequate signal-to-noise ratios must be ensured for the measurements at all frequencies employed.

Simultaneous TS measurements at three frequencies (using two split-beam and one single-beam transducers) were made possible by utilizing positional information from a split-beam system to beam-compensate the data from an adjacent single-beam system. Differences in the resulting multiple-frequency TS measurements provided information about the identity of constituents in a mixed-species assembly. It should be noted, however, that the imprecision in single-frequency TS measurements is compounded in the estimation of TS and S_v differences. This measurement uncertainty, thresholding effects, and especially the sparse spectral sampling will limit the power of this taxa identification method.

The ultimate utilities of both the multi-frequency method for *in situ* TS measurements and the TS differences technique for taxa identification depend upon the uncertainty in the basic measurements. For example, the filtering efficiency of target matches at multiple-frequencies depends upon: (1) precise estimates of $\hat{\alpha}$, $\hat{\beta}$, and $\hat{r}$; (2) parallel beam axes or an accurate transform function; (3) low noise; and (4) low target complexity and narrow receiver bandwidth. This is illustrated through the simulation results (Fig. 1), which shows that the multi-frequency method is most efficient if the angular discrepancy between the two frequency detections is tightly constrained.

The angular resolution is a function of the phase quantization of the echosounder and the angle sensitivity of the transducer [Eq. (3)]. In turn, the angle sensitivity is dependent upon the transducer shading (Wilson, 1988; Foote, 1990) and the acoustic wavelength. Therefore, tolerances in the transducer manufacturing may produce inequities between the theoretical d_{eff} and the realized effective spacing. In addition, a change in the sound speed will result in the same percentage change in λ and Λ. Judging from these studies, the precision of the angular measurements (α and β) due to variances in d_{eff} and wavelength were approximately ± 0.26 degrees for the Simrad ES38-12 and ± 0.14 degrees for the ES120-7.

Optimally, the transducers should be mounted so the beams are projecting parallel to one another. If the actual angle discrepancies change as a function of range, the transducer geometry in Fig. 7 is not accurate and Eq. (17) must be appropriately modified (see Fig. 15). One method is to determine a spatial transform equation for each of the transducer pairs by moving a target within the overlapping beams and recording the associated spatial information (α, β, and r).

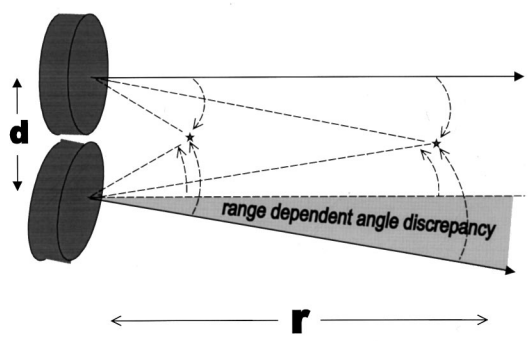

FIG. 15. Angle discrepancy as a function of range for nonparallel beams. For the multiple-frequency method, the transducers should optimally be mounted so the beams are projecting parallel to one another. If the beams are not parallel in both the alongship and athwartship planes, it is necessary to derive a spatial transform equation for each of the transducer pairs using the target positional data (α, β, and r) collected while moving an object within the overlapping beams.

Using the EK500, the maximum angular precision is noise limited at SNR less than 24 dB [Eqs. (6) and (17)]. As seen in Fig. 13, nearly all of the matching field measurements had larger SNRs and were therefore not noise limited. It is also important to note that the maximum angle discrepancy in the two-frequency method was 1.5 degrees ($\sim$6.7 phase steps for the ES38-12), or approximately seven times the angle discrepancy which could be attributed to noise. This implies that precise angular matching, and consequently the efficacy of the multi-frequency TS detection method, is limited by some process other than noise.

The multi-frequency method has the potential to greatly improve the accuracy and precision of *in situ* TS measurements by efficiently filtering multiple-target interference events which tend to pass the single-frequency algorithm. The realized effectiveness of the method is primarily dependent upon the minimum angular discrepancy criteria that can be imposed without filtering valid single targets. In these studies, the minimum angular discrepancy criteria was not limited by echosounder phase quantization, parallelism of the transducer beams, nor ambient noise. Therefore, by deduction, the method is likely limited by target complexity and the finite receiver bandwidths.

Echosounder designs and deployment configurations include many competing considerations, one of which is the effect of narrow-bandwidth receiver filters on both the SNR and the measured echo amplitude and phase. In general, near-optimal SNR can be achieved with receiver bandpass filters of width$=2/\tau$. The tradeoff is an echo signal with amplitude and phase that are functions of the bandpass filter—especially for narrower bandwidth filters. For pulses of 1 and 0.3 ms, the optimal filter bandwidths are 2 and 6.7 kHz, respectively. Unfortunately, the echosounder receiver bandwidths are user selectable to be either 1% or 10% of the transmit frequency. Because TS measurements were the priority of these experiments, and because the EK500 uses measurements of peak echo amplitude to estimate TS, ''wide''

bandpass filters ($BW = 0.1f$) were chosen. Consequently, the receiver bandwidths were 79% to 90% wider than optimal from a SNR perspective.

With appreciable bandwidth, narrow-band assumptions are not necessarily valid and the received signal $[p(t)]$ is derived from the complex transmit signal $[S(\omega)]$, the polychromatic backscattering amplitude of the acoustic scatterer $[F(\omega)]$, and the frequency response function of the receiver $[H(\omega)]$:

$$p(t) = \mathrm{FT}^{-1}(\mathrm{SFH}), \tag{20}$$

where the Fourier transform operator FT^{-1} transforms the argument from the frequency to the time domains (Foote, 1983). Because scattering is a stochastic process, the amplitude and phase of $p(t)$ can vary over time and frequency. This variability appears to be the limiting factor in the efficiency of the multi-frequency TS detection method. It also has ramifications for increased uncertainty in beam compensation of TS measurements in a split-beam system. Moreover, with the increasing development and usage of broadband acoustic systems (e.g., Simmonds *et al.*, 1996) for the purposes of TS measurements (e.g., Martin *et al.*, 1996), scatterer classification (e.g., Zakharia *et al.*, 1996) and also echo-integration (e.g., Thompson and Love, 1996), additional constraints due to the stochastic nature of scattering may be realized.

A very promising extension of this multi-frequency TS measurement method involves the synchronized usage of three or more collocated echosounders, at least two split-beam systems and another with very high range resolution. For example, if simultaneous transmissions were made at 38, 120, and 200 kHz with pulse lengths of 1.0, 0.3, and 0.06 ms, respectively, echoes are only accepted as individual targets if (1) the scatter is coherent at both 38 and 120 kHz and (2) the 200-kHz system ($c\tau/2 \cong 0.045$ m) does not resolve more than one target within the coincident sampling volumes. In this way, improvements are made to both the phase and range discriminators for multiple-target rejection.

ACKNOWLEDGMENTS

This research was supported by the U.S. Antarctic Marine Living Resources Program (AMLR) and the SFRI. Special thanks go to Manuel Barange, SFRI, and Merrick Whittle, IMT, for graciously funding and accommodating the test tank experiments, and to Valerie Loeb, Moss Landing Marine Laboratories, and Wesley Armstrong, AMLR, for summarizing the net sampling data. Thanks go to Tim Stanton, Woods Hole Oceanographic Institution, for advice and encouragement; to George Watters, International Tropical Tuna Commission, for discussions on noise statistics; and to three anonymous reviewers for constructive critiques.

AMLR (**1997**). *1996/97 Field Season Report: Objectives, Accomplishments, and Tentative Conclusions*, edited by J. Rosenberg, SWFSC Admin. Rep. LJ-97-09.

Bodholt, H., Nes, H., and Solli, H. (**1983**). *A new echo-sounder system for fish abundance estimation and fishery research*, ICES Council Meeting 1988 (collected papers) (ICES, Copenhagen, Denmark).

Bodholt, H. (**1990**). *Fish density derived from echo-integration and in-situ target strength measurements*, ICES Council Meeting 1990 (collected papers) (ICES, Copenhagen, Denmark).

Bodholt, H. (**1991**). ''Split-beam transducer for target strength measurement,'' in *Scandinavian Cooperation Meeting in Acoustics XIII*, edited by H. Hobæk, Department of Physics Sci./Tech. Rep. 227 (University of Bergen, Bergen, Norway), p. 73.

Bodholt, H., and Solli, H. (**1992**). ''Application of the split-beam technique for *in-situ* target strength measurements,'' World Fisheries Congress, Athens.

Brierly, A. S., Ward, P., Watkins, J. L., and Goss, C. (**1998**). ''Acoustic discrimination of Southern Ocean zooplankton,'' Deep Sea Res. II **45(7)**, 1155–1173.

Chu, D., Stanton, T. K., and Wiebe, P. H. (**1992**). ''Frequency dependence of sound backscattering from live individual zooplankton,'' ICES J. Mar. Sci., **49**, 97–106.

Demer, D. A. (**1994**). ''Accuracy and precision of acoustic surveys of Antarctic krill,'' Ph.D. thesis, UCSD.

Demer, D. A., and Martin, L. V. (**1995**). ''Zooplankton target strength: Volumetric or areal dependence?'' J. Acoust. Soc. Am. **98**, 1111–1118.

Devereaux, R. F. (**1953**). ''Isaacs-Kidd midwater trawl,'' Scripps Institution of Oceanography, Refer. 53–3.

Ehrenberg, J. E. (**1979**). ''A comparative analysis of *in situ* methods for directly measuring the acoustic target strength of individual fish,'' IEEE J. Ocean Eng. **OE-4**, 141–152.

Ehrenberg, J. E. (**1989**), ''A Review of Target Strength Estimation Techniques,'' in *Underwater Acoustic Data Processing* (Kluwer, Boston), pp. 161–175.

Fernandes, P. G., and Simmonds, E. J. (**1996**). ''Practical approaches to account for receiver delay and the TVG start time in the calibration of the Simrad EK500,'' ICES C. M. B:17, 8 pp (mimeo).

Foote, K. G. (**1983**). ''Maintaining precision calibrations with optimal copper spheres,'' J. Acoust. Soc. Am. **73**, 1054–1063.

Foote, K. G. (**1990**). ''Spheres for calibrating an eleven-frequency acoustic measurement system,'' ICES J. Mar. Sci. **46**, 284–286.

Foote, K. G. (**1991**). ''Summary of methods for determining fish target strength at ultrasonic frequencies,'' ICES J. Mar. Sci. **48**, 211–217.

Foote, K. G. (**1996**). ''Coincidence echo statistics,'' J. Acoust. Soc. Am. **99**, 266–271.

Greenlaw, C. F. (**1979**). ''Acoustical estimation of zooplankton populations,'' Limnol. Oceanogr. **24**, 226–242.

Greenlaw, C. F., and Johnson, R. K. (**1983**). ''Multiple-frequency Acoustical Estimation,'' Biol. Oceanogr. **2**, 227–252.

Hewitt, R. P., and Demer, D. A. (**1991**). ''Krill abundance,'' Nature (London), **353**, 310.

Hewitt, R. P., and Demer, D. A. (**1993**). ''Dispersion and abundance of Antarctic krill in the vicinity of Elephant Island in the 1992 austral summer,'' Mar. Ecol. Prog. Ser. **99**, 29–39.

Holliday, D. V. (**1977**). ''Extracting bio-physical information from the acoustic signatures of marine organisms,'' in *Oceanic Sound Scattering Prediction*, edited by N. R. Andersen and B. J. Zahuranec (Plenum, New York).

Kerr, D. E. (**1988**). *Propagation of Short Radio Waves* (McGraw-Hill, New York, 1951), reprinted (Peninsula, Los Altos, CA).

MacLennan, D. N. (**1987**). ''Time-varied-gain functions for pulsed sonars,'' J. Sound Vib. **110**, 511–522.

MacLennan, D. N., and Simmonds, E. J. (**1992**). *Fisheries Acoustics* (Chapman and Hill, London).

Madureira, L. S. P., Ward, P., and Atkinson, A. (**1993**). ''Differences in backscattering strength determined at 120 and 38 kHz for three species of Antarctic macroplankton,'' Mar. Ecol. Prog. Ser. **93**, 17–24.

Martin, L. V., Stanton, T. K., Wiebe, P. H., and Lynch, J. F. (**1996**). ''Acoustic classification of zooplankton,'' ICES J. Mar. Sci. **53**(2), 217–224.

Medwin, H., and Clay, C. S. (**1998**). *Fundamentals of Acoustical Oceanography* (Academic, San Diego).

Rice, J. A. (**1988**). *Mathematical Statistics and Data Analysis* (Duxbury Press, Belmont, CA).

Senturia, S. D. and Wedlock, B. D. (**1975**). *Electronic Circuits and Applications* (Wiley, New York).

Simmonds, E. J., Armstrong, F., and Copland, P. J. (**1996**). ''Species identification using wideband backscatter with neural network and discriminant analysis,'' ICES J. Mar. Sci. **53**(2), 189–196.

Simrad (**1996**). ''Simrad EK500 Scientific Echo Sounder Instruction Manual,'' Simrad Subsea A/S, Horten, Norway.
Soule, M. A., Barange, M., and Hampton, I. (**1995**) ''Evidence of bias in estimates of target strength obtained with a split-beam echo-sounder,'' ICES J. Mar. Sci. **52**, 139–144.
Soule, M. A., Hampton, I., and Barange, M. (**1996**). ''Potential improvements to current methods of recognizing single targets with a split-beam echo-sounder,'' ICES J. Mar. Sci. **53**, 237–243.
Soule, M. A., Barange, M., Solli, H., and Hampton, I. (**1997**). ''Performance of a new phase algorithm for discriminating between single and overlapping echoes in a split-beam echo-sounder,'' ICES J. Mar. Sci. **54**, 934–938.
Stanton, T. K., Wiebe, P. H., Chu, D., Benfield, M., Scanlon, L., Martin, L. V., and Eastwood, R. L. (**1994**). ''On acoustic estimates of zooplankton biomass,'' ICES J. Mar. Sci. **51**, 505–512.
Thompson, C. H., and Love, R. H. (**1996**). ''Determination of fish size distributions and areal densities using broadband low-frequency measurements,'' ICES J. Mar. Sci. **53**(2), 197–202.
Wilson, O. B. (**1988**). *Introduction to Theory and Design of Sonar Transducers* (Peninsula, Los Altos, CA).
Zakharia, M. E., Magand, F., Hetroit, F., and Diner, N. (**1996**). ''Wideband sounder for fish species identification at sea,'' ICES J. Mar. Sci. **53**(2), 203–208.